Please cite this article in press as: Osman and Pek, A sisRNA/miRNA Axis Prevents Loss of Germline Stem Cells during Starvation in *Drosophila*, Stem Cell Reports (2018), https://doi.org/10.1016/j.stemcr.2018.06.002

Stem Cell Reports
Report
ISSCR
OPEN ACCESS

A sisRNA/miRNA Axis Prevents Loss of Germline Stem Cells during Starvation in *Drosophila*

Ismail Osman[1,2] and Jun Wei Pek[1,*]
[1]Temasek Life Sciences Laboratory, National University of Singapore, 1 Research Link, Singapore 117604, Singapore
[2]Department of Biological Sciences, National University of Singapore, Singapore 117543, Singapore
*Correspondence: junwei@tll.org.sg
https://doi.org/10.1016/j.stemcr.2018.06.002

SUMMARY

Animal reproduction responds to nutritional status. During starvation, *Drosophila* and *Caenorhabditis elegans* enter a period of reproductive diapause with increase apoptosis, while maintaining a stable pool of germline stem cells (GSCs). How GSCs are protected is not understood. Here, we show that a sisRNA/miRNA axis maintains ovarian GSCs during starvation in *Drosophila*. Starvation induces the expression of an ovary-enriched sisRNA *sisR-2*, which negatively regulates GSC maintenance via a fatty acid metabolism gene *dFAR1*. *sisR-2* promotes the expression of *bantam*, which in turn inhibits the activity of *sisR-2*, forming a negative feedback loop. Therefore, *bantam* acts as a buffer to counteract *sisR-2* activity to prevent GSC loss during starvation. We propose that the *sisR-2/bantam* axis confers robustness to GSCs in *Drosophila*.

INTRODUCTION

Noncoding RNAs (ncRNAs) have emerged as important players in gene regulation (Cech and Steitz, 2014; Kung et al., 2013; Rinn and Chang, 2012; Ghildiyal and Zamore, 2009; Matera et al., 2007). Recently, stable intronic sequence RNA (sisRNA) has been discovered in several organisms such as viruses, yeast, *Drosophila*, *Xenopus*, and mammals (Osman et al., 2016; Pek and Okamura, 2015). We are only beginning to appreciate the biological significance of these intronic transcripts, which are proposed to function as an added layer of gene regulation. sisRNAs have been suggested to regulate expression of their parental genes (host genes where the sisRNAs originate from), act as molecular sponges for proteins and microRNAs (miRNAs), and play a role in translational regulation (Osman et al., 2016). In *Drosophila*, two sisRNAs, *sisR-1* and *sisR-4*, have been reported to regulate the expression of their parental genes (Pek, 2018; Tay and Pek, 2017; Pek et al., 2015). It remains unclear whether sisRNAs also engage in other forms of feedback loops to modulate gene expression. On the other hand, miRNAs are small ncRNAs that play important roles in many biological processes by regulating the expression of their target genes post-transcriptionally (Bushati and Cohen, 2007). They are often engaged in regulatory feedback/feedforward loops to fine-tune gene expression, and confer robustness in response to stress (Posadas and Carthew, 2014; Ebert and Sharp, 2012; Herranz and Cohen, 2010). Regulatory crosstalks between sisRNAs and miRNAs have not been reported.

Reproduction is highly sensitive to changes in nutritional status. Some organisms have evolved to reduce their reproductive capacity as a way to conserve resources (Tatar et al., 2001). Studies in the nematode worm *Caenorhabditis elegans* and *Drosophila* had revealed that, during starvation, animals enter a period of reproductive diapause that halts germline activity (Angelo and Van Gilst, 2009; Drummond-Barbosa and Spradling, 2001). In both cases, although much of the germline undergoes apoptosis, there is little or no loss of germline stem cells (GSCs). The molecular pathways ensuring the protection of GSCs under starvation are poorly understood. Currently, ncRNAs such as *bantam*, *miR-184*, *sisR-1*, and Piwi-interacting RNAs are known to play intrinsic roles in the regulation of GSC maintenance (Rojas-Ríos et al., 2017; Wong et al., 2017; Iovino et al., 2009; Yang et al., 2009; Shcherbata et al., 2007). Whether ncRNA regulatory axes confer robustness in GSCs is not explored.

RESULTS

sisR-2 Regulates the Number of GSCs

We focused on *sisR-2*, an ovary-enriched sisRNA from the *mushroom bodies tiny* (*mbt*) gene locus (Ng et al., 2018; Pek et al., 2015). To examine the function of *sisR-2*, we cloned the full-length sequence of *sisR-2* by performing 5′ and 3′ rapid amplification of cDNA ends (Figures 1A and S1A) and generated two independent transgenic shRNA flies (Figure 1A). Using a germline-specific driver, knockdown was specific to *sisR-2* but not the parental gene *mbt* mRNA or the Mbt protein (Figures S1B and S1C). Furthermore, RNAi against the *mbt* exon reduced *mbt* mRNA level but had no effect on the abundance of *sisR-2* (Figures 1A and S1B). These results demonstrate that *sisR-2* RNAi was specific to *sisR-2* and did not target the *mbt* pre-mRNA.

Knockdown of *sisR-2* using both RNAi lines resulted in a significant increase in the number of eggs laid per female

This is an open access article under the CC BY-NC-ND license (http://creativecommons.org/licenses/by-nc-nd/4.0/).

Please cite this article in press as: Osman and Pek, A sisRNA/miRNA Axis Prevents Loss of Germline Stem Cells during Starvation in *Drosophila*, Stem Cell Reports (2018), https://doi.org/10.1016/j.stemcr.2018.06.002

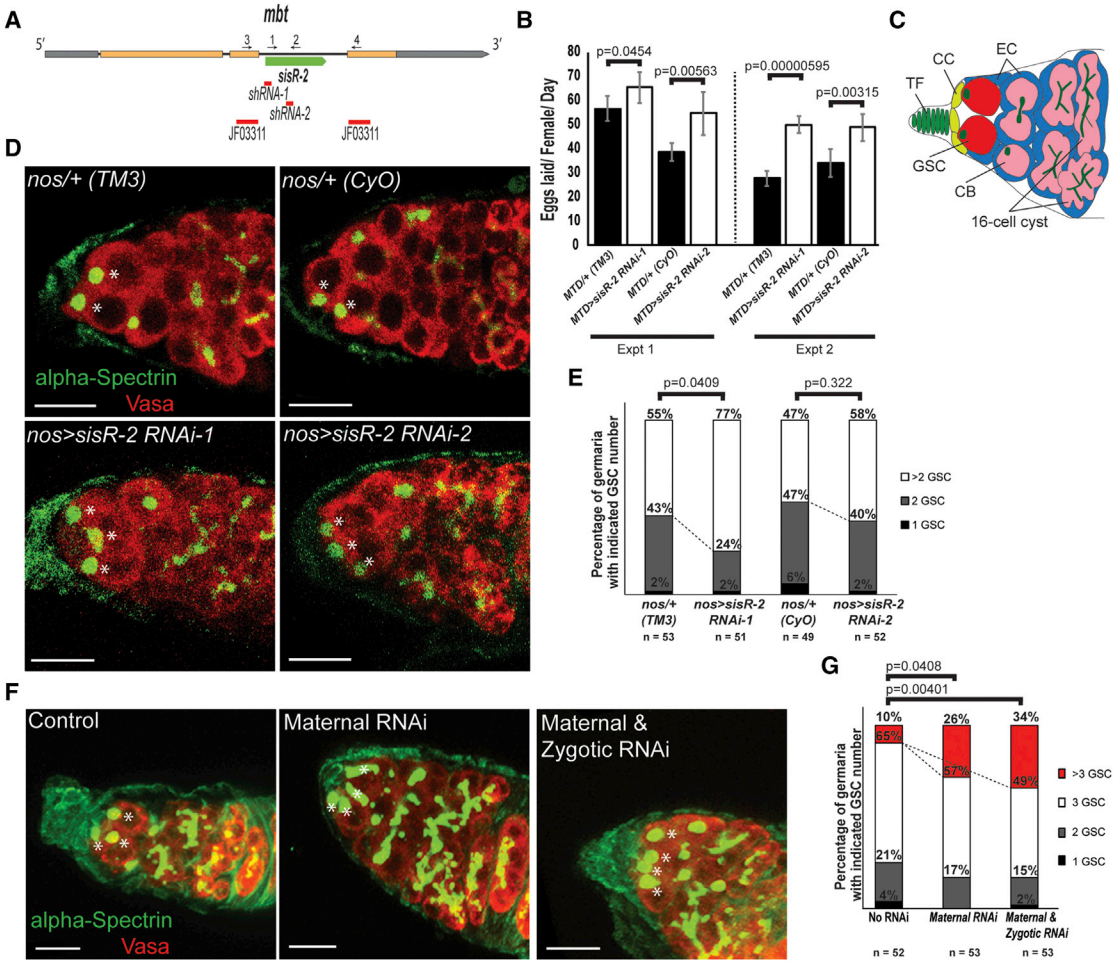


Figure 1. *sisR-2* Regulates the Number of GSCs

(A) The *mbt* locus showing the regions of *sisR-2*, primers, targeted by RNAi and shRNA constructs.

(B) Chart showing the number of eggs laid per female per day for the indicated genotypes. Data from two sets of experiments are shown. Student's t test was performed. Error bars depict SD. N = 5 biological replicates.

(C) Diagram showing the cell types in a *Drosophila* germarium in the ovary. TF, terminal filament; CC, cap cells; GSC, germline stem cells; EC, escort cells; CB, cystoblasts.

(D) Confocal images showing the germaria of the indicated genotypes stained with α-Spectrin (green) and Vasa (red).

(E) Chart showing the percentage of germaria with the indicated number of GSCs in different genotypes shown in (D). Fisher's exact test was performed. N = 49–53 germaria.

(F) Confocal images showing the germaria of the indicated genotypes with α-Spectrin (green) and Vasa (red). Undriven parental *sisR-2* shRNA-1 flies were used as the control.

(G) Chart showing the percentage of germaria with the indicated number of GSCs in different genotypes shown in (F). Fisher's exact test was performed. N = 52–53 germaria.

GSCs are marked by asterisks (*). Scale bars, 10 μm.

compared with sibling controls (Figure 1B), suggesting a role in oogenesis. The *Drosophila* ovary consists of several ovarioles, which are strings of progressively developing egg chambers. These egg chambers originate from the germarium, located at the anterior end of the ovariole. The anterior tip of the germarium contains two to three GSCs that can be identified by their location next to the cap cells and the presence of spherical spectrosomes (visualized using HTS or α-Spectrin staining) (Figure 1C) (Kai and Spradling, 2003). To understand how *sisR-2* regulates egg production, we first counted the number of ovarioles in the *sisR-2* RNAi flies, and did not observe any significant differences (Figure S1D). By staining with antibodies against α-Spectrin and Vasa (a germline marker), we observed an

Please cite this article in press as: Osman and Pek, A sisRNA/miRNA Axis Prevents Loss of Germline Stem Cells during Starvation in *Drosophila*, Stem Cell Reports (2018), https://doi.org/10.1016/j.stemcr.2018.06.002

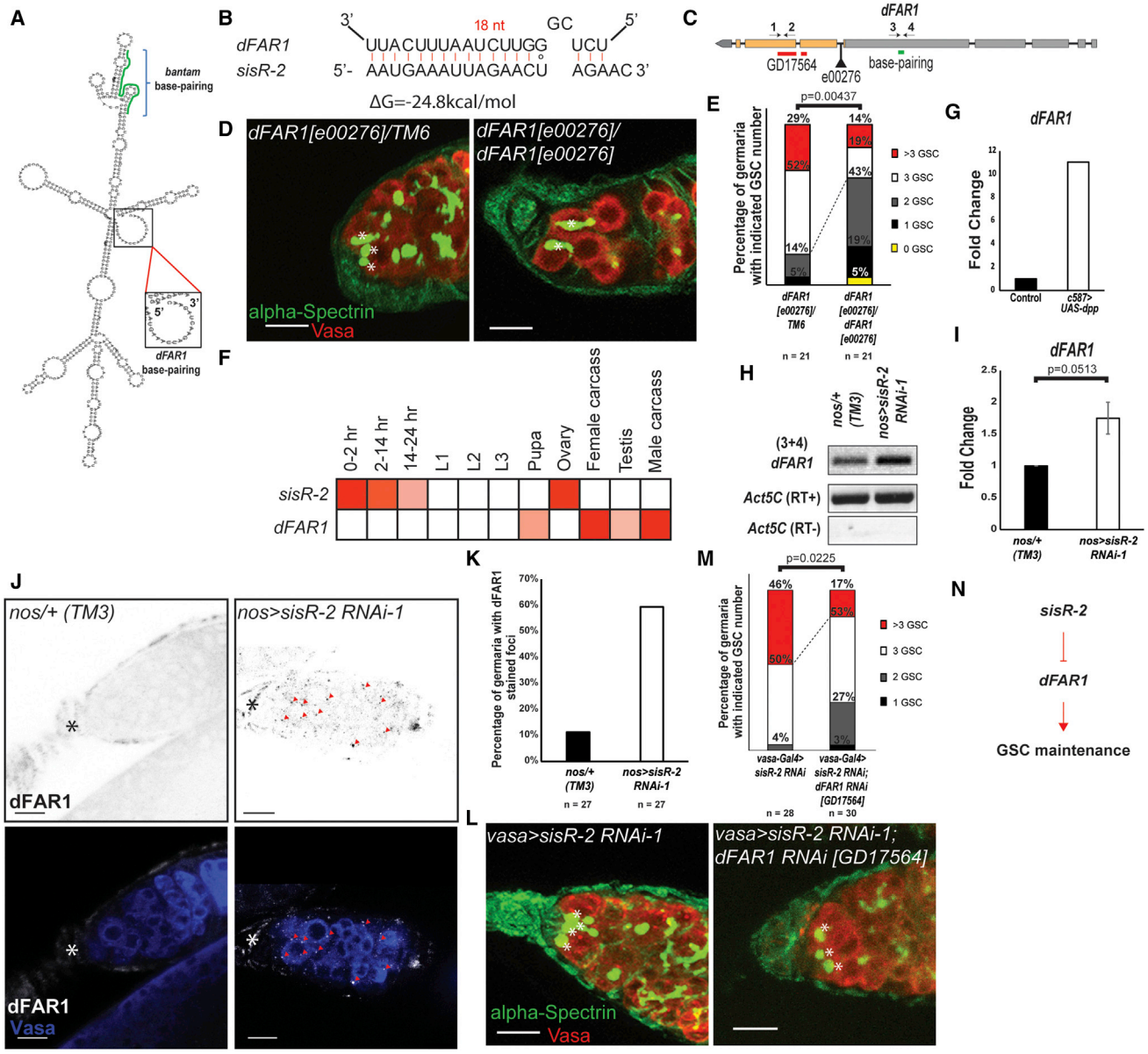


Figure 2. *sisR-2* Regulates GSC Maintenance via *dFAR1*

(A) Predicted secondary structure of *sisR-2*. Regions that base pair with *dFAR1* and *bantam* are indicated.

(B) Sequence of the exposed 3′ end tail of *sisR-2*, indicating potential base pairing with *dFAR1*.

(C) The *dFAR1* locus showing regions of predicted *sisR-2* base pairing, primers, transposon insertion (mutant), and targeted by RNAi construct.

(D and L) Confocal images showing the germaria of the indicated genotypes with α-Spectrin (green) and Vasa (red).

(E and M) Chart showing the percentage of germaria with the indicated number of GSCs in different genotypes shown in (D and L), respectively. Fisher's exact test was performed. N = 21–30 germaria.

(F) Heatmap showing the relative levels of *sisR-2* and *dFAR1*. Red, high expression; white, low or undetectable expression.

(G) qPCR showing the relative levels of *dFAR1* in ovaries of the indicated genotypes.

(H) Representative RT-PCR showing the levels of *dFAR1* in ovaries of *sisR-2* RNAi flies.

(I) Graph showing the relative levels of *dFAR1* normalized to *act5C*, as shown in (H). Student's t test was performed. Error bars depict SD. N = 3 biological replicates.

(legend continued on next page)

increase in the number of germaria with more GSCs in *sisR-2* RNAi ovaries (Figures 1D and 1E). We only counted GSCs that were in close contact with the cap cells, to avoid including the cystoblasts that also contain spectrosomes (Figure 1C). In *nos > sisR-2 RNAi-1* ovaries, 77% of the germaria counted had >2 GSCs, compared with only 55% in *nos/+ (TM3)* control ovaries. Similarly, in *nos > sisR-2 RNAi-2* ovaries, 58% of the germaria counted had >2 GSCs, as compared with only 47% in *nos/+ (CyO)* control ovaries (Figures 1D and 1E). Consistently, by using pMad, a marker for active bone morphogenetic protein signaling in GSCs, we observed more germaria with increased pMad-positive GSCs in *sisR-2* RNAi ovaries (Figures S1E and S1F). Furthermore, the expression of *sisR-2* was upregulated in cystoblasts (*bam* mutants) when compared with GSCs (*dpp* overexpression), consistent with a role in promoting GSC differentiation (Figures S1G and S1H). Taken together, we conclude that *sisR-2* negatively regulates GSC maintenance.

As *sisR-2* is maternally deposited into *Drosophila* oocytes, we asked if maternal *sisR-2* also functions to regulate the number of GSCs in the progeny (Pek et al., 2015). We first generated a stable stock of *sisR-2* RNAi flies, whereby females from this stock would deposit reduced levels of *sisR-2* into their oocytes. We crossed these females with wild-type males and counted the number of GSCs in their female progeny (Figure S1I). Flies with reduced levels of maternally deposited *sisR-2* (maternal RNAi only) had an increase in GSCs (Figures 1F, 1G, and S1I). Interestingly, zygotic knockdown of *sisR-2* in these flies (maternal and zygotic RNAi) had an additive increase in the number of GSCs (Figures 1F and 1G), suggesting that both maternal and zygotic *sisR-2* functions to repress GSC number.

sisR-2 Regulates GSC Maintenance via *dFAR1*

To characterize the molecular function of *sisR-2*, we predicted its secondary structure using the Vienna RNAfold software. *sisR-2* was predicted to form a secondary structure with a protected 5′ end consisting of several stable hairpins and an exposed 3′ end tail (Figure 2A). The secondary structure is consistent with a distinct 5′ end and heterogeneous 3′ ends (Figure S1A). The predicted structure of *sisR-2* resembles that of *sisR-1*, which represses the ncRNA *ASTR*, possibly via base pairing of its 3′ tail with the target (Wong et al., 2017; Pek et al., 2015). We hypothesized that *sisR-2* may also regulate its target gene(s) in a similar manner. By performing a BLAST search, we found that the 20-nucleotide 3′ end of *sisR-2* can form an 18-nucleotide base pairing with the internal untranslated region of the bi-cistronic transcript encoding the protein coding genes *CG10096* and *CG10097* (Figures 2A–2C and S2A). Using the RNAhybrid program, we confirmed the stability of this base pairing with a minimum free energy of −24.8 kcal/mol (Figure 2B) (Rehmsmeier et al., 2004).

CG10096 and *CG10097* are highly similar genes with ~50% identity. For our analysis, we focused on *CG10096* because of the availability of mutants for genetic analysis. *CG10096* is one of several *Drosophila* homologs identified for the two human *fatty-acyl-CoA reductase* (*FAR*) genes, *FAR1* and *FAR2*, which are involved in ether lipid synthesis in the peroxisomes (Faust et al., 2012). We therefore named *CG10096* as *dFAR1*. We first asked if *dFAR1* plays a role in the regulation of GSCs. *dFAR1* homozygous mutants displayed a GSC loss phenotype suggesting that *dFAR1* regulates GSC maintenance (Figures 2D, 2E, and S2B). Since *sisR-2* exhibit spatial and temporal expression patterns (Pek et al., 2015), we next asked if its predicted target, *dFAR1* display reciprocal expression patterns. We made use of the modENCODE temporal and tissue expression data in FlyBase, and observed that *dFAR1* exhibited a mutually exclusive temporal and spatial expression patterns to *sisR-2*, suggesting that *sisR-2* negatively regulates *dFAR1* (Figure 2F). We then verified that *dFAR1* is indeed present in GSC-like cells by examining the levels of *dFAR1* in the ovaries overexpressing *dpp* (Figure S1H). Expression of *dFAR1* is higher in the ovaries overexpressing *dpp* compared with control whole ovaries, indicating that *sisR-2* and *dFAR1* are co-expressed in the same cells (Figure 2G). To investigate whether *sisR-2* regulates *dFAR1 in vivo*, we examined the levels of *dFAR1* in the ovaries of *sisR-2* RNAi flies. Knockdown of *sisR-2* resulted in an upregulation of *dFAR1* mRNA in the ovaries (Figures 2H and 2I). Since the FAR1 proteins in humans and *Drosophila* show substantial similarity (Figure S2C), we used antibodies raised against a peptide containing residues 7–149 of human FAR1 to investigate the levels of dFAR1 in *sisR-2* RNAi flies (Figure S2C). A reduced amount of dFAR1 protein was detected in *dFAR1* homozygous mutants, indicating that the human FAR1 antibody is able to detect dFAR1 (Figure S2D). Using this human FAR1 antibody, we observed an increase in the number of dFAR1 foci in the germaria of *sisR-2* RNAi flies compared with controls (Figures 2J and 2K). In addition, the level of dFAR1 protein was also higher in *sisR-2*

(J) Confocal images showing the germaria of the indicated genotypes stained with dFAR1 (black/white) and Vasa (blue). Arrowheads, dFAR1 foci. Asterisks, germarium anterior.

(K) Chart showing the percentage of germaria with dFAR1 foci in the different genotypes shown in (J). N = 27 germaria.

(N) Working model.

GSCs are marked by asterisks (*). Scale bars, 10 μm.

Please cite this article in press as: Osman and Pek, A sisRNA/miRNA Axis Prevents Loss of Germline Stem Cells during Starvation in *Drosophila*, Stem Cell Reports (2018), https://doi.org/10.1016/j.stemcr.2018.06.002

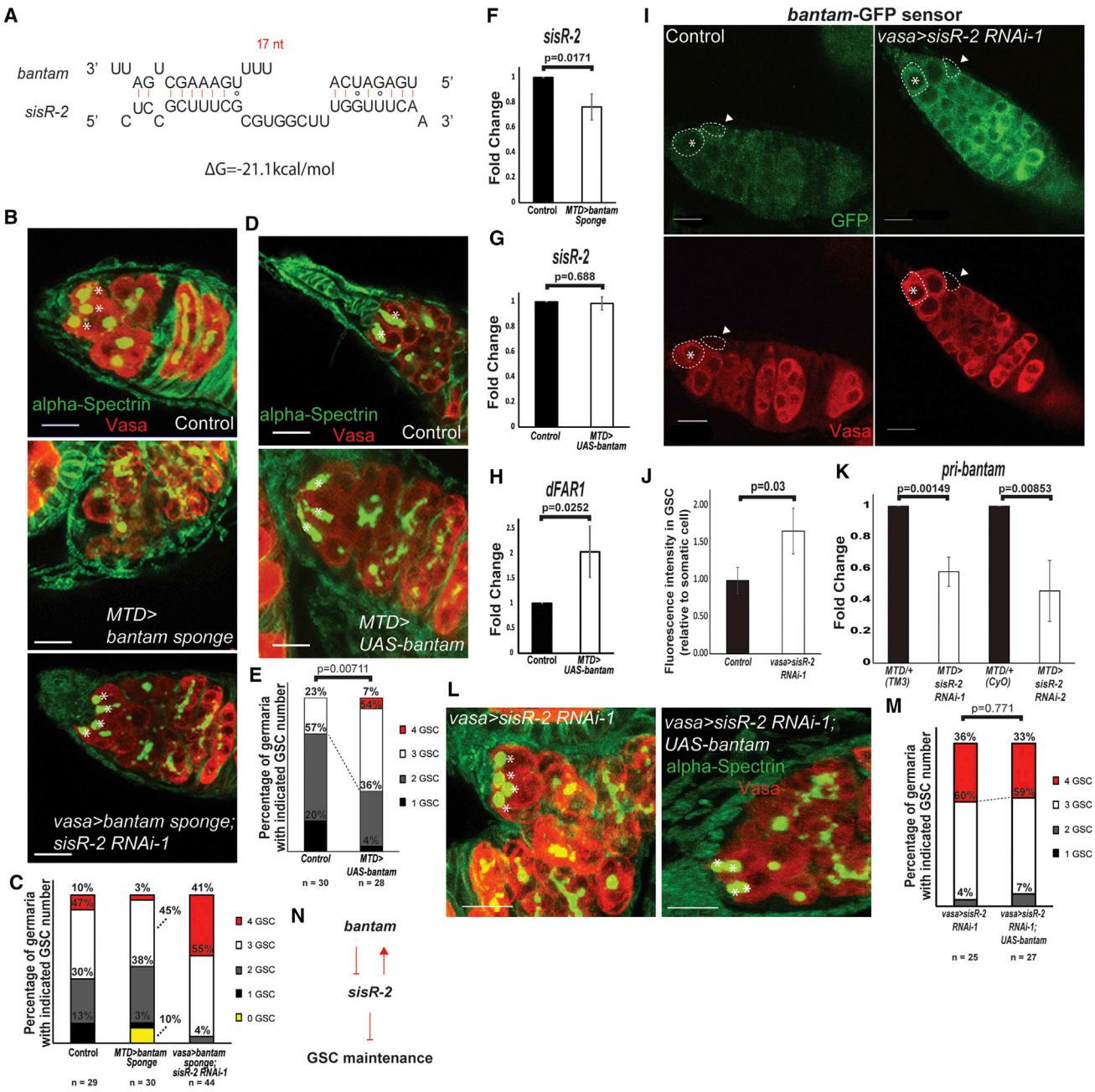


Figure 3. *bantam* Regulates GSC Maintenance by Repressing *sisR-2* Activity

(A) Sequence of *bantam* indicating potential base pairing with *sisR-2*.

(B and D) Confocal images showing the germaria of the indicated genotypes with α-Spectrin (green) and Vasa (red).

(C and E) Chart showing the percentage of germaria with the indicated number of GSCs in different genotypes shown in (B and D), respectively. Fisher's exact test was performed in (E). N = 28–44 germaria.

(F and G) qPCR showing the relative levels of *sisR-2* in ovaries of the indicated genotypes. Student's t test was performed. Error bars depict SD. N = 3 biological replicates.

(H) qPCR showing the relative levels of *dFAR1* in ovaries of the indicated genotypes. Student's t test was performed. Error bars depict SD. N = 3 biological replicates.

(I) Confocal images showing the germaria of the indicated genotypes stained with GFP (green) and Vasa (red). Asterisks, GSCs. Arrowheads, somatic cells.

(legend continued on next page)

RNAi ovaries (Figure S2D). Together, these results indicate that *sisR-2* downregulates *dFAR1* in the ovaries.

We next examined if *sisR-2* regulates GSC maintenance by repressing *dFAR1*. Using an RNAi line (GD17564) designed to target two exons of *dFAR1* (Figures 2C and S2E), we found that knockdown of *dFAR1* could rescue the GSC phenotype in *sisR-2* RNAi flies (Figures 2L and 2M). In contrast, no significant difference in GSC number was observed in the ovaries of *dFAR1* knockdown flies in otherwise wild-type background compared with control (Figures S2F and S2G), confirming a specific genetic interaction between *sisR-2* and *dFAR1*. Taken together, our data suggest that *sisR-2* controls the number of GSCs in *Drosophila* by modulating *dFAR1* (Figure 2N).

bantam Regulates GSC Maintenance by Repressing *sisR-2* Activity

Since both sisRNAs and miRNAs are engaged in self-regulatory feedback loops, we considered the possibility of a *sisR-2*/miRNA axis (Tay and Pek, 2017; Pek et al., 2015; Posadas and Carthew, 2014; Ebert and Sharp, 2012; Herranz and Cohen, 2010). *bantam* has been reported to play a role in the maintenance of GSCs in the ovaries (Yang et al., 2009; Shcherbata et al., 2007). We identified a potential 17-nucleotide stable base pairing between *bantam* and *sisR-2* (Figures 2A and 3A). Unlike canonical seed base pairing, the predicted interaction between *bantam* and *sisR-2* is non-canonical, containing two G:U wobble base pairs. We first verified the cell-autonomous role of *bantam* in GSCs using transgenic flies expressing *bantam* sponge. Germline expression of *bantam* sponge led to the occurrence of germaria with no GSCs (Figures 3B and 3C). Conversely, germline overexpression of *bantam* resulted in an increase in the number of GSCs (Figures 3D and 3E). Thus, *bantam* plays a cell-autonomous role in maintaining GSCs.

We hypothesized that *bantam* may promote GSC maintenance by repressing the activity of *sisR-2*. Knockdown of *sisR-2* could rescue the GSC loss phenotype observed in the *bantam* sponge flies, confirming that *sisR-2* acts downstream of *bantam* in the regulation of GSCs (Figures 3B and 3C). Consistent with recent reports that non-canonical base pairing does not lead to target degradation (Gilot et al., 2017; Agarwal et al., 2015), we did not observe any up- or downregulation of *sisR-2* in ovaries expressing *bantam* sponge or *bantam*, respectively (Figures 3F and 3G). These results suggest that *bantam* inhibits the activity, but not the abundance, of *sisR-2*. Furthermore, we observed an increase in *dFAR1* levels in the ovaries of flies overexpressing *bantam* (Figure 3H). Our results are consistent with a model that *bantam* promotes GSCs by repressing the activity of *sisR-2* (Figure 3N).

Next, we wondered if *sisR-2* reciprocally regulates *bantam*, forming a feedback loop. By using a *bantam* sensor transgene to monitor the activity of *bantam*, we observed an increase in GFP signal in *sisR-2* RNAi ovaries, indicating a reduction in *bantam* activity (Figures 3I, 3J, and S3). Similarly, knockdown of *sisR-2* resulted in a downregulation of the primary *bantam* transcript in the ovaries, indicating that *sisR-2* promotes the transcription of *bantam* (Figure 3K). We then asked if *bantam* acts downstream of *sisR-2* in the regulation of GSCs. Overexpression of *bantam* was not able to enhance the GSC phenotype in *sisR-2* RNAi flies (Figures 3L and 3M), thus consistent with our data that *bantam* acts upstream of *sisR-2* in regulating GSCs (Figure 3N). Altogether, our data support a model for a *sisR-2*/*bantam* axis in the control of GSC maintenance (Figure 3N).

sisR-2/bantam Axis Protects GSCs from Starvation

During nutrient deprivation, *Drosophila* females exhibit a marked reduction in the rate of egg production. This is largely due to a drop in the rate of germline cell proliferation coupled with an increase in apoptosis at two checkpoints during oogenesis (Drummond-Barbosa and Spradling, 2001). The number of GSCs, however, remains unchanged, suggesting the presence of a mechanism that prevents loss of GSCs during starvation. We investigated the possibility that the *sisR-2*/*bantam* axis functions to protect GSCs during starvation. We monitored the expression of *sisR-2* and *bantam* in ovaries of *y w* flies that were starved or fed with yeast. Interestingly, expressions of *sisR-2* and *bantam* were both elevated in the ovaries of starved flies (Figures 4A, 4B, and S4A), while that of another germline-specific gene *nanos* was unchanged (Figure S4B), indicating that the activity of the *sisR-2/bantam* axis was upregulated during starvation. Interestingly, the expression of *dFAR1* remained relatively unchanged (Figure S4C). We hypothesized that

(J) Chart quantifying the fluorescence intensity in GSCs of the indicated genotypes shown in (I). Student's t test was performed. Error bars depict SD. N = 3 germaria.
(K) qPCR showing the relative levels of *pri-bantam* in ovaries of *sisR-2* RNAi flies. Student's t test was performed. Error bars depict SD. N = 3 biological replicates.
(L) Confocal images showing the germaria of the indicated genotypes with α-Spectrin (green) and Vasa (red).
(M) Chart showing the percentage of germaria with the indicated number of GSCs in different genotypes shown in (L). Fisher's exact test was performed. N = 25–27 germaria.
(N) Working model.
GSCs are marked by asterisks (*). Scale bars, 10 μm.

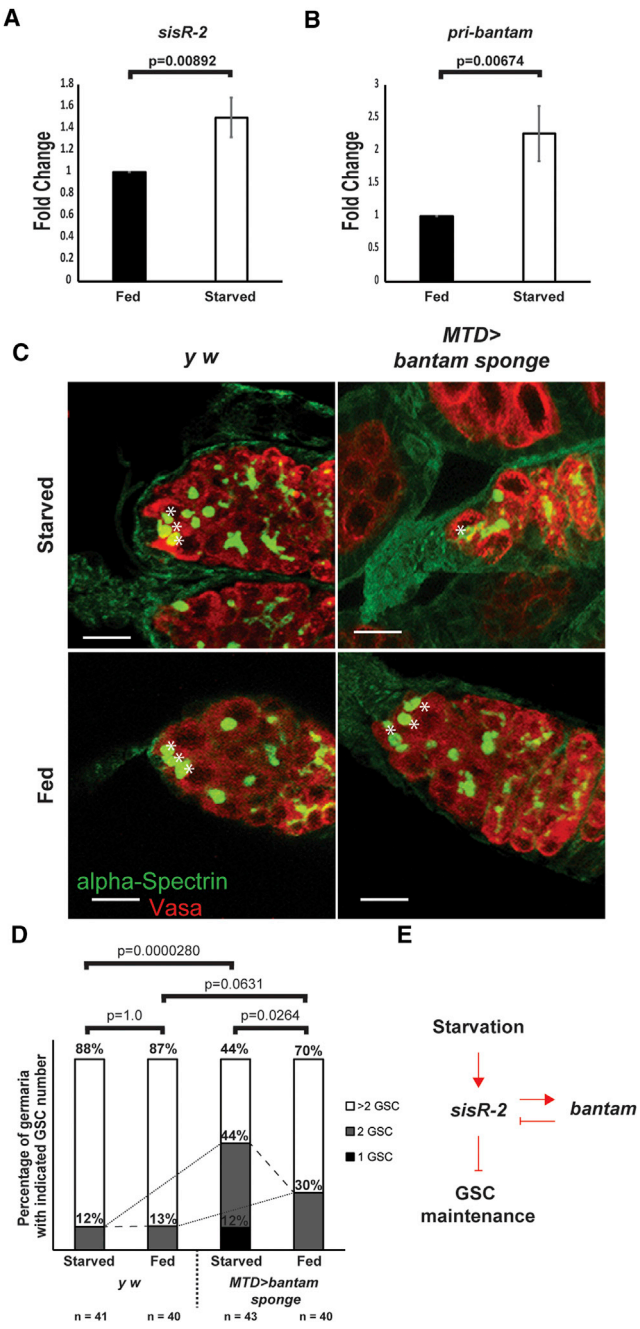


Figure 4. *sisR-2/bantam* Axis Protects GSCs from Starvation

(A and B) qPCR showing the relative levels of (A) *sisR-2* and (B) *pri-bantam* in ovaries of *y w* flies raised in fed or starved conditions. Student's t test was performed. Error bars depict SD. N = 3 biological replicates.

(C) Confocal images showing the germaria of the indicated genotypes, raised in fed or starved conditions, with α-Spectrin (green) and Vasa (red).

(D) Chart showing the percentage of germaria with the indicated number of GSCs in different genotypes shown in (C). Fisher's exact test was performed. N = 40–43 germaria.

(E) Proposed model.

GSCs are marked by asterisks (*). Scale bars, 10 μm.

bantam acts as a buffer to counteract *sisR-2* activity, thus preventing the repression of dFAR1 and the loss of GSCs during starvation. Consistent with previous reports, the number of GSCs in starved and fed *y w* flies had no significant differences (Figures 4C and 4D). Instead, *bantam* sponge flies were more sensitive to starvation by exhibiting a significant decrease in the number of GSCs (Figures 4C and 4D). As *sisR-2* is upregulated during starvation, we wondered if flies overexpressing *sisR-2* also display increased sensitivity to starvation. Indeed, we observed a decrease in the number of GSCs in flies overexpressing *sisR-2* during starvation (Figures S4D–S4G). However, this decrease was not statistically significant, possibly due to the still intact negative feedback by *bantam* acting on *sisR-2* in these flies (Figure 4E).

DISCUSSION

In summary, we have shown that the *sisR-2/bantam* feedback axis plays an important role in maintaining GSCs during starvation (Figure 4E). We show that *sisR-2* regulates GSCs by modulating *dFAR1*. The functions of *FAR* genes in *Drosophila* have not been extensively characterized (Faust et al., 2012). *dFAR1* is predicted to encode a peroxisomal protein that modulates fatty acid metabolism. This is particularly interesting in the light that fatty acid metabolism protects GSC loss during starvation in *C. elegans* (Angelo and Van Gilst, 2009), suggesting that lipid metabolism is a conserved downstream pathway.

In many animals, the highly conserved insulin-signaling pathway is responsible for coordinating changes in nutrition to the metabolic status and growth of the organism (Shim et al., 2013). In *Drosophila*, *Drosophila* insulin-like peptides (DILPs) are secreted by the brain in response to food. The *Drosophila* female germline is highly sensitive to changes in diet, and this is regulated partly via insulin signaling, which has been shown to promote both the maintenance and proliferation of GSCs (Hsu and Drummond-Barbosa, 2009). Since *sisR-2* is elevated during starvation, whereas DILPs expression is reduced, it is tempting to speculate that the expression of *sisR-2* is repressed by the insulin-signaling pathway.

One possible mode of *sisR-2* action is to regulate *dFAR1* mRNA decay and/or translation. Moreover, *bantam* may bind and regulate the activity of *sisR-2* by remodeling *sisR-2*'s secondary structure. Finally, our study provides a paradigm for a negative feedback mechanism involving a miRNA and a sisRNA in preventing the loss of GSCs during nutritional stress. Analogous RNA/RNA regulatory crosstalks may be conserved in other species.

EXPERIMENTAL PROCEDURES

A detailed description of all methods is included in the Supplemental Information.

Fly Strains

Flies were maintained in standard cornmeal medium at 25°C. The following Gal4 drivers were used to drive UAS-transgene expression in the germline: *MTD-Gal4* (Petrella et al., 2007), *nanos-Gal4-VP16* (Van Doren et al., 1998), and *vasa-Gal4* (gift from Y. Yamashita). *Mbt* RNAi (JF03311), and *dFAR1[e00276]* were obtained from the Bloomington Stock Center. *dFAR1* RNAi (GD17564) was obtained from Vienna Drosophila Resource Center. *Bam[Δ86]*, *c587-Gal4*, and *UAS-dpp* were gifts from Y. Cai. *UAS-bantam* sponge, *UAS-bantam.D*, and *bantam* sensor were gifts from S. Cohen (Herranz et al., 2012; Brennecke et al., 2003). For collection of eggs, virgin females were fed with wet yeast for several days. For starvation experiments, newly eclosed flies were kept in vials containing 1% agarose, either fed with wet yeast or starved, for 3 days. Generation of dsRed-intron-myc overexpression flies was done as described previously (Pek et al., 2015). For generation of *sisR-2* shRNA transgenic flies, shRNAs targeting *sisR-2* were designed and cloned into Valium22 plasmid, performed as described previously (Ni et al., 2011). Sequences were chosen to avoid potentially off-target effects. Transgenic flies were generated by Genetic Services using phiC31 integrase-mediated insertion into 25C7 and 68A4 landing site (Bischof et al., 2007). Oligonucleotides sequences are available in Table S1. To compare the expression of *sisR-2* between GSCs and the differentiated CBs, we used ovaries with tumorous germaria from *c587>UAS-dpp* and *bam[Δ86]/bam[Δ86]* flies. In *c587>UAS-dpp* flies, the tumorous germarium is filled with GSC-like cells (due to an expansion in niche signaling throughout the germarium) (Kai and Spradling, 2003; Xie and Spradling, 1998). *bam[Δ86]/bam[Δ86]* mutant flies also contain a tumorous germarium; however, their germarium is filled with CB-like cells instead. These cells are more like CBs as they are no longer receiving niche signals as they have left the niche, but they remain as single spectrosome cells as the differentiation program in these cells cannot be turned on without bam expression (Chen and McKearin, 2003).

Immunostaining

Immunostaining was performed as described previously (Wong et al., 2017; Pek and Kai, 2011). Ovaries were fixed in a solution of 16% paraformaldehyde and Grace's medium at a ratio of 2:1 for 20 min, rinsed, and washed with PBX solution (PBS containing 0.2% Triton X-100) three times for 10 min each, and pre-absorbed for 30 min in PBX containing 5% normal goat serum. Ovaries were incubated overnight with primary antibodies at room temperature, washed three times for 20 min each with PBX before a 4 hr incubation with secondary antibodies at room temperature. Ovaries were again washed three times for 20 min each with PBX. Primary antibodies used in this study are as follows: mouse monoclonal anti-α-Spectrin (3A9, 1:1; Developmental Studies Hybridoma Bank), guinea pig anti-Vasa (1:1,000) (Patil and Kai, 2010), rabbit anti-pMad (1:50; Cell Signaling Technology, cat. no. 9516), mouse anti-GFP (1:500, Invitrogen, monoclonal 3×10^6, cat. no. A-11120), and rabbit anti-human FAR1 (1:100; Sigma-Aldrich, cat. no. HPA017322). Images were taken with a Carl Zeiss LSM 5 Exciter Upright microscope and processed using Adobe Photoshop.

Identification of GSCs

GSCs were identified based on the following criteria: presence of Vasa staining, position at the anterior tip of the germarium, next to the cap cells, and the presence of a single spherical spectrosome stained using anti-α-Spectrin antibodies.

SUPPLEMENTAL INFORMATION

Supplemental Information includes Supplemental Experimental Procedures, four figures, and one table and can be found with this article online at https://doi.org/10.1016/j.stemcr.2018.06.002.

AUTHOR CONTRIBUTIONS

I.O. and J.W.P. conceived the project, performed the experiments, and wrote the paper.

ACKNOWLEDGMENTS

We thank Y. Cai, S. Cohen, J. Gall, T. Kai, T. Raabe, Y. Yamashita, the Developmental Studies Hybridoma Bank, the Vienna Drosophila Resource Center, and the Bloomington Stock Center for reagents; and K. Okamura, N. Tolwinski, and M. Tay for discussion. The authors are supported by the Temasek Life Sciences Laboratory.

Received: March 3, 2018
Revised: June 4, 2018
Accepted: June 4, 2018
Published: June 28, 2018

REFERENCES

Agarwal, V., Bell, G.W., Nam, J.W., and Bartel, D.P. (2015). Predicting effective microRNA target sites in mammalian mRNAs. Elife *4*. https://doi.org/10.7554/eLife.05005.

Angelo, G., and Van Gilst, M.R. (2009). Starvation protects germline stem cells and extends reproductive longevity in *C. elegans*. Science *326*, 954–958.

Bischof, J., Maeda, R.K., Hediger, M., Karch, F., and Basler, K. (2007). An optimized transgenesis system for *Drosophila* using germ-line-specific φC31 integrases. Proc. Natl. Acad. Sci. USA *104*, 3312–3317.

Brennecke, J., Hipfner, D.R., Stark, A., Russell, R.B., and Cohen, S.M. (2003). Bantam encodes a developmentally regulated microRNA that controls cell proliferation and regulates the proapoptotic gene hid in *Drosophila*. Cell *113*, 25–36.

Bushati, N., and Cohen, S.M. (2007). microRNA functions. Annu. Rev. Cell Dev. Biol. *23*, 175–205.

Cech, T.R., and Steitz, J.A. (2014). The noncoding RNA revolution-trashing old rules to forge new ones. Cell *157*, 77–94.

Chen, D., and McKearin, D. (2003). Dpp signaling silences bam transcription directly to establish asymmetric divisions of germline stem cells. Curr. Biol. *13*, 1786–1791.

Drummond-Barbosa, D., and Spradling, A.C. (2001). Stem cells and their progeny respond to nutritional changes during *Drosophila* oogenesis. Dev. Biol. *231*, 265–278.

Ebert, M.S., and Sharp, P.A. (2012). Roles for microRNAs in conferring robustness to biological processes. Cell *149*, 515–524.

Faust, J.E., Verma, A., Peng, C., and McNew, J.A. (2012). An inventory of peroxisomal proteins and pathways in *Drosophila melanogaster*. Traffic *13*, 1378–1392.

Ghildiyal, M., and Zamore, P.D. (2009). Small silencing RNAs: an expanding universe. Nat. Rev. Genet. *10*, 94–108.

Gilot, D., Migault, M., Bachelot, L., Journe, F., Rogiers, A., Donnou-Fournet, E., Mogha, A., Mouchet, N., Pinel-Marie, M.L., Mari, B., et al. (2017). A non-coding function of TYRP1 mRNA promotes melanoma growth. Nat. Cell Biol. *19*, 1348–1357.

Herranz, H., and Cohen, S.M. (2010). MicroRNAs and gene regulatory networks: managing the impact of noise in biological systems. Genes Dev. *24*, 1339–1344.

Herranz, H., Hong, X., and Cohen, S.M. (2012). Mutual repression by bantam miRNA and Capicua links the EGFR/MAPK and Hippo pathways in growth control. Curr. Biol. *22*, 651–657.

Hsu, H.-J., and Drummond-Barbosa, D. (2009). Insulin levels control female germline stem cell maintenance via the niche in *Drosophila*. Proc. Natl. Acad. Sci. USA *106*, 1117–1121.

Iovino, N., Pane, A., and Gaul, U. (2009). miR-184 has multiple roles in *Drosophila* female germline development. Dev. Cell *17*, 123–133.

Kai, T., and Spradling, A. (2003). An empty *Drosophila* stem cell niche reactivates the proliferation of ectopic cells. Proc. Natl. Acad. Sci. USA *100*, 4633–4638.

Kung, J.T., Colognori, D., and Lee, J.T. (2013). Long noncoding RNAs: past, present, and future. Genetics *193*, 651–669.

Matera, A.G., Terns, R.M., and Terns, M.P. (2007). Non-coding RNAs: lessons from the small nuclear and small nucleolar RNAs. Nat. Rev. Mol. Cell Biol. *8*, 209–220.

Ng, S.S.J., Zheng, R.T., Osman, I., and Pek, J.W. (2018). Generation of *Drosophila* sisRNAs by independent transcription from cognate introns. iScience *4*, 68–75.

Ni, J.-Q., Zhou, R., Czech, B., Liu, L.-P., Holderbaum, L., Yang-Zhou, D., Shim, H.-S., Tao, R., Handler, D., Karpowicz, P., et al. (2011). A genome-scale shRNA resource for transgenic RNAi in *Drosophila*. Nat. Methods *8*, 405–407.

Osman, I., Tay, M.L., and Pek, J.W. (2016). Stable intronic sequence RNAs (sisRNAs): a new layer of gene regulation. Cell. Mol. Life Sci. *73*, 3507–3519.

Patil, V.S., and Kai, T. (2010). Repression of retroelements in *Drosophila* germline via piRNA pathway by the tudor domain protein tejas. Curr. Biol. *20*, 724–730.

Pek, J.W. (2018). Stable intronic sequence RNAs engage in feedback loops. Trends Genet. *34*, 330–332.

Pek, J.W., and Kai, T. (2011). A role for vasa in regulating mitotic chromosome condensation in *Drosophila*. Curr. Biol. *21*, 39–44.

Pek, J.W., and Okamura, K. (2015). Regulatory RNAs discovered in unexpected places. Wiley Interdiscip. Rev. RNA *6*, 671–686.

Pek, J.W., Osman, I., Tay, M.L., and Zheng, R.T. (2015). Stable intronic sequence RNAs have possible regulatory roles in *Drosophila melanogaster*. J. Cell Biol. *211*, 243–251.

Petrella, L.N., Smith-Leiker, T., and Cooley, L. (2007). The ovhts polyprotein is cleaved to produce fusome and ring canal proteins required for *Drosophila* oogenesis. Development *134*, 703–712.

Posadas, D.M., and Carthew, R.W. (2014). MicroRNAs and their roles in developmental canalization. Curr. Opin. Genet. Dev. *27*, 1–6.

Rehmsmeier, M., Steffen, P., Hochsmann, M., and Giegerich, R. (2004). Fast and effective prediction of microRNA/target duplexes. RNA *10*, 1507–1517.

Rinn, J.L., and Chang, H.Y. (2012). Genome regulation by long noncoding RNAs. Annu. Rev. Biochem. *81*, 145–166.

Rojas-Ríos, P., Chartier, A., Pierson, S., and Simonelig, M. (2017). Aubergine and piRNAs promote germline stem cell self-renewal by repressing the proto-oncogene Cbl. EMBO J. *36*, 3194–3211.

Shcherbata, H.R., Ward, E.J., Fischer, K.A., Yu, J.-Y., Reynolds, S.H., Chen, C.-H., Xu, P., Hay, B.A., and Ruohola-Baker, H. (2007). Stage-specific differences in the requirements for germline stem cell maintenance in the *Drosophila* ovary. Cell Stem Cell *1*, 698–709.

Shim, J., Gururaja-Rao, S., and Banerjee, U. (2013). Nutritional regulation of stem and progenitor cells in *Drosophila*. Development *140*, 4647–4656.

Tatar, M., Kopelman, A., Epstein, D., Tu, M.-P., Yin, C.-M., and Garofalo, R. (2001). A mutant *Drosophila* insulin receptor homolog that extends life-span and impairs neuroendocrine function. Science *292*, 107–110.

Tay, M.L., and Pek, J.W. (2017). Maternally inherited stable intronic sequence RNA triggers a self-reinforcing feedback loop during development. Curr. Biol. *27*, 1062–1067.

Van Doren, M., Williamson, A.L., and Lehmann, R. (1998). Regulation of zygotic gene expression in *Drosophila* primordial germ cells. Curr. Biol. *8*, 243–246.

Wong, J.T., Akhbar, F., Ng, A.Y.E., Tay, M.L., Loi, G.J.E., and Pek, J.W. (2017). DIP1 modulates stem cell homeostasis in *Drosophila* through regulation of sisR-1. Nat. Commun. *8*, 759.

Xie, T., and Spradling, A.C. (1998). Decapentaplegic is essential for the maintenance and division of germline stem cells in the *Drosophila* ovary. Cell *94*, 251–260.

Yang, Y., Xu, S., Xia, L., Wang, J., Wen, S., Jin, P., and Chen, D. (2009). The bantam microRNA is associated with *Drosophila* fragile x mental retardation protein and regulates the fate of germline stem cells. PLoS Genet. *5*, e1000444.

Stem Cell Reports, Volume *11*

Supplemental Information

A sisRNA/miRNA Axis Prevents Loss of Germline Stem Cells during Starvation in *Drosophila*

Ismail Osman and Jun Wei Pek

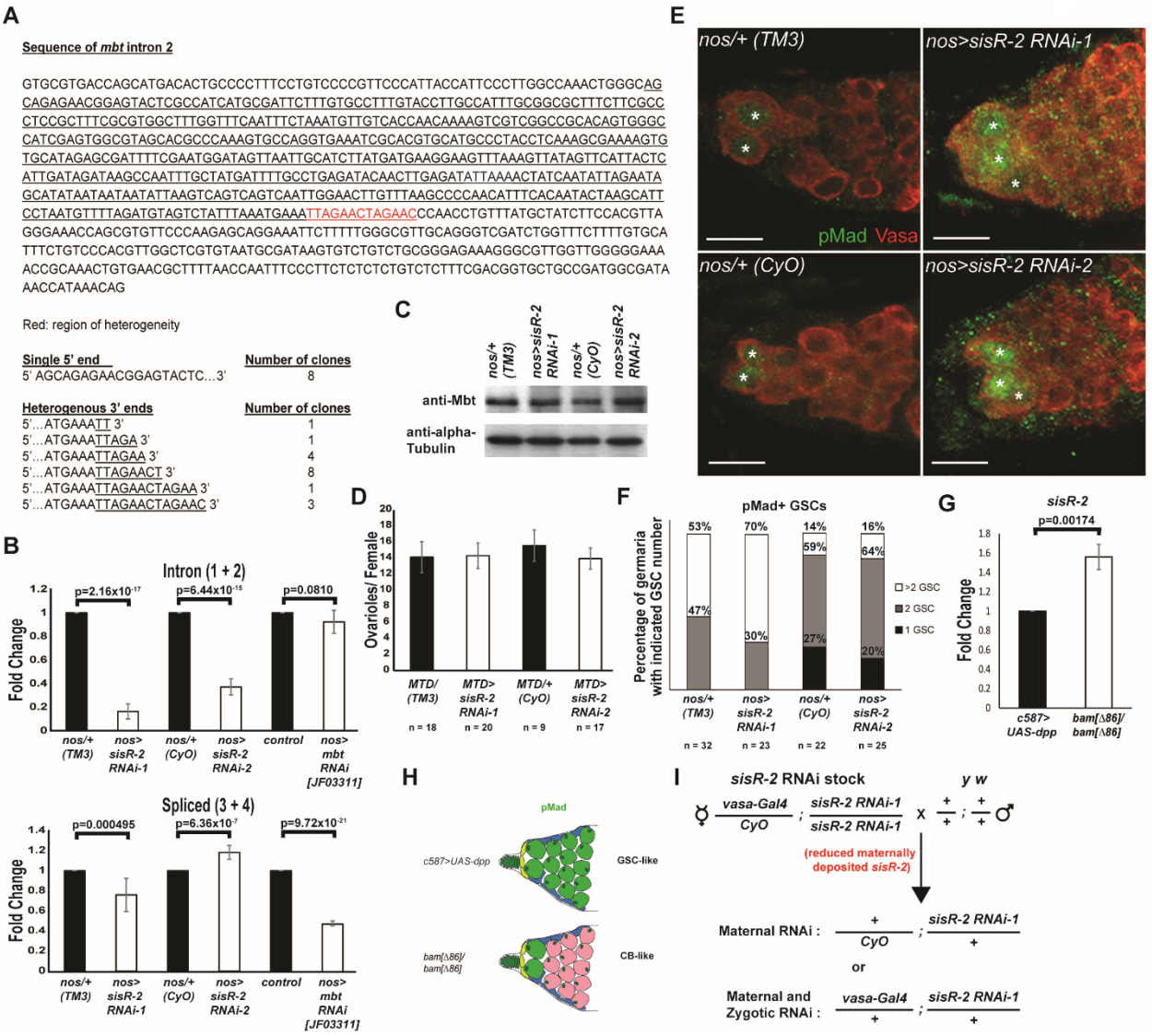


Figure S1. Characterization of *sisR-2*. Related to Figure 1. (**A**) Full sequence of the *mbt* second intron, with the sequence of *sisR-2* underlined. (**B**) qPCR showing the relative levels of *sisR-2* and spliced *mbt* in ovaries of the indicated genotypes. Student's t-test was performed. Error bars depict S.D. N = 3 biological replicates. (**C**) Western blot showing the level of Mbt protein in ovaries of control and *sisR-2* RNAi flies. (**D**) Chart showing the number of ovarioles per female in control and *sisR-2* RNAi flies. Error bars depict S.D. N = 9-20 ovaries. (**E**) Confocal images showing the germaria of the indicated genotypes stained with pMad (green) and Vasa (red). (**F**) Chart showing the percentage of germaria with the indicated number of GSCs in different genotypes shown in (E). N = 22-32 germaria. (**G**) qPCR showing the relative levels of *sisR-2* in ovaries of the indicated genotypes. Student's t-test was performed. Error bars depict S.D. N = 3 biological replicates. (**H**) Diagram illustrating the difference between the two tumorous germaria of the indicated genotypes. (**I**) Cross scheme for maternal and zygotic knockdown of *sisR-2*. GSCs were marked by asterisks (*). Scale bar: 10 μm.

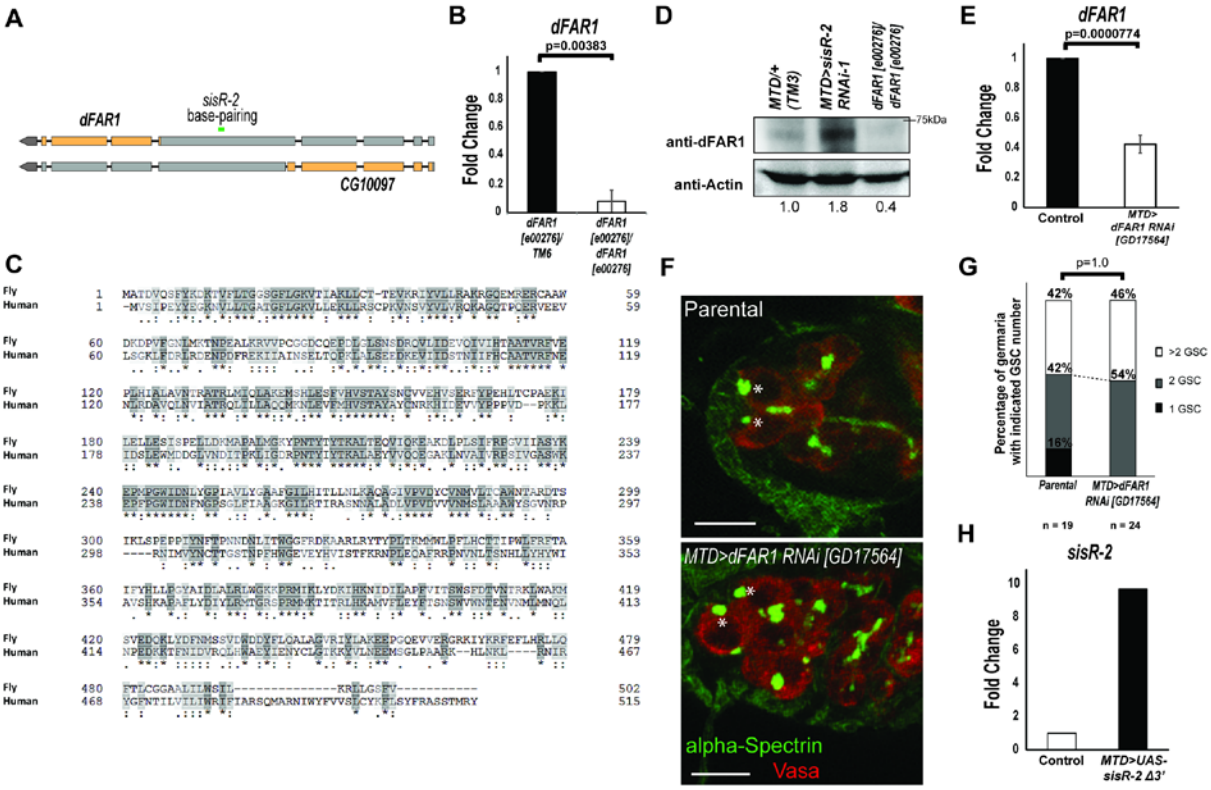


Figure S2. Characterization of *dFAR1* mutants and RNAi flies. Related to Figure 2. (**A**) The *dFAR1* locus showing the region of a paralogous upstream gene *CG10097*. (**B and E**) qPCR showing the relative levels of *dFAR1* in ovaries of the indicated genotypes. Student's t-test was performed. Error bars depict S.D. N = 3 biological replicates. (**C**) Alignment of fly and human FAR1 proteins showing regions of sequence similarity. (**D**) Western blot showing the level of dFAR1 protein in ovaries of the indicated genotypes. Numbers below indicate relative band intensities of dFAR1 normalized to Actin. (**F**) Confocal images showing the germaria of the indicated genotypes stained with alpha-Spectrin (green) and Vasa (red). (**G**) Chart showing the percentage of germaria with the indicated number of GSCs in different genotypes shown in (F). Fisher's exact test was performed. N = 19-24 germaria. (**H**) qPCR showing the relative levels of *sisR-2* in ovaries of the indicated genotypes. GSCs were marked by asterisks (*). Scale bar: 10 μm.

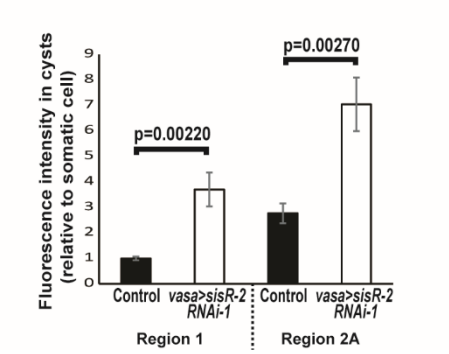


Figure S3. Characterization of *bantam* GFP sensor in *sisR-2* RNAi ovaries. Related to Figure 3. Chart quantifying the fluorescence intensity in cysts, from regions 1 and 2A of the germarium, of the indicated genotypes shown in Figure 3(H). Student's t-test was performed. Error bars depict S.D. N = 3 germaria.

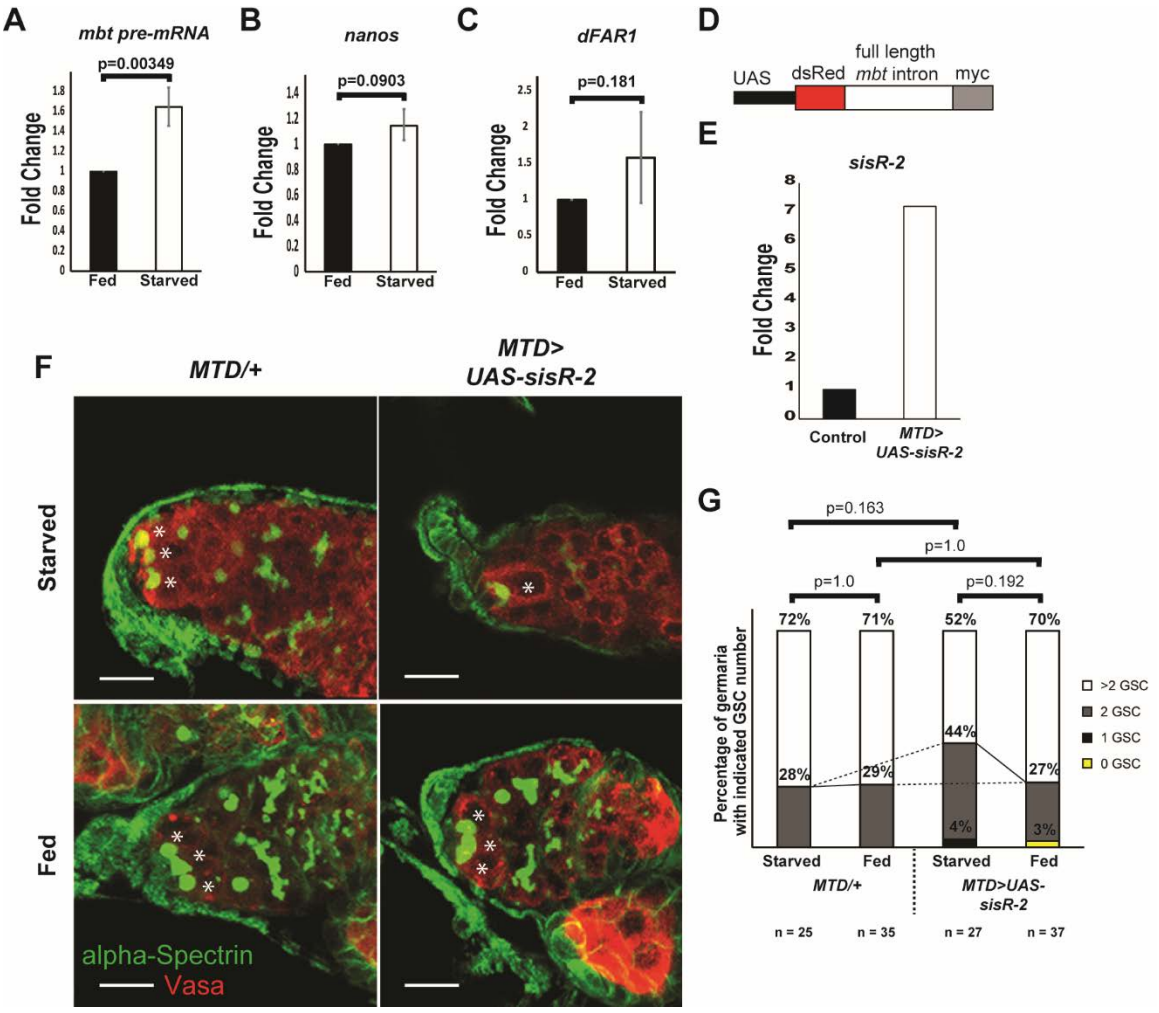


Figure S4. Changes in gene expression in ovaries, and GSC counts in *sisR-2* overexpressing flies, under fed or starved conditions. Related to Figure 4. (**A-C**) qPCR showing the relative levels of (A) *mbt* pre-mRNA, (B) *nanos* and (C) *dFAR1* in ovaries of *y w* flies raised in fed or starved conditions. Student's t-test was performed. Error bars depict S.D. N = 3 biological replicates. (**D**) Construct used to express *sisR-2*. (**E**) qPCR showing the relative levels of *sisR-2* in ovaries of the indicated genotypes. (**F**) Confocal images showing the germaria of the indicated genotypes, raised in fed or starved conditions, with alpha-Spectrin (green) and Vasa (red). (**G**) Chart showing the percentage of germaria with the indicated number of GSCs in different genotypes shown in (D). Fisher's exact test was performed. N = 25-37 germaria.

Table S1. List of oligonucleotides used.

mbt 5' RACE RT	TCAAGTTGTATCTCAGGCAAAAT
mbt 3' RACE RT	GCGAGCACAGAATTAATACGACTCACTATAGGTTTTTTTTTTTTVN
mbt 5' RACE 1st Nested PCR Fw	CACACTTTTCGCTTTGAGGTA
mbt 5' RACE 1st Nested PCR Rv	GCGAGCACAGAATTAATACGACTCACTATAGGAAAAAAAAAAAAVN
mbt 5' RACE 2nd Nested PCR Fw	ACATTTAGAAATTGAAACCAAAGC
mbt 5' RACE 2nd Nested PCR Rv	CGCGGATCCGAATTAATACGACTCACTATAGG
mbt 3' RACE 1st Nested PCR Fw1	GCTTTGGTTTCAATTTCTAAATGT
mbt 3' RACE 1st Nested PCR Fw2	TACCTCAAAGCGAAAAGTGTG
mbt 3' RACE 1st Nested PCR Rv	GCGAGCACAGAATTAATACGACT
mbt 3' RACE 2nd Nested PCR Fw1	TACCTCAAAGCGAAAAGTGTG
mbt 3' RACE 2nd Nested PCR Fw2	ATTTTGCCTGAGATACAACTTGA
mbt 3' RACE 2nd Nested PCR Rv	CGCGGATCCGAATTAATACGACTCACTATAGG
mbt shRNA-1 top oligo	CTAGCAGTGGCAGCAGAGAACGGAGTACTTAGTTATATTCAAGCATAAG TACTCCGTTCTCTGCTGCCGCG
mbt shRNA-1 bottom oligo	AATTCGCGGCAGCAGAGAACGGAGTACTTATGCTTGAATATAACTAAGT ACTCCGTTCTCTGCTGCCACTG
mbt shRNA-2 top oligo	CTAGCAGTGGTGAAATCGCACGTGCATGCTAGTTATATTCAAGCATAGC ATGCACGTGCGATTTCACCGCG
mbt shRNA-2 bottom oligo	AATTCGCGGTGAAATCGCACGTGCATGCTATGCTTGAATATAACTAGCA TGCACGTGCGATTTCACCACTG
mbt intron Fw	CCATCATGCGATTCTTTGTG
mbt intron Rv	GATTTCACCTGGCACTTTGG
mbt spliced Fw	GGACGAGGAGCAGATAGCC
mbt spliced Rv	CATCTCGATGACCATGATGC
mbt pre-mRNA Fw	CGC AAA CTG TGA ACG CTT TT
mbt pre-mRNA Rv	GAT AGC TTC ACG CGA CCA TC
actin5C Fw	TGCCCATCTACGAGGGTTAT
actin5C Rv	GTACTTGCGCTCTGGCGG
actin5C qPCR Fw	TGCCCATCTACGAGGGTTATG
actin5C qPCR Rv	CAGAGTACTTGCGCTCTGGCGG

dFAR1 5’ UTR Fw	AATCGAAGCTTGTTCGAACT
dFAR1 5’ UTR Rv	CTTAGGTGTCAAGTGGCGTG
dFAR1 exon Fw	TACGGACCCATTGCAGTTCT
dFAR1 exon Rv	TGATACTTGTATCCCGGGCC
pri-bantam Fw	CGCTCAGATGCAGATGTTGTTGATG
pri-bantam Rv	ATCGGAATGTGGAATGTGGTATTCATTG
nanos spliced Fw	CACTGTGTCCACCAATCTCG
nanos spliced Rv	CTCGCACTGAGTGGCTATTG

Supplemental experimental procedures

RNA extraction

Tissues were homogenized in 1.5 ml Eppendorf tubes using a plastic pestle and RNA was extracted using the TRIzol extraction protocol (Ambion) or the Direct-zol RNA miniprep kit (Zymo Research). For RACE, rRNA depletion was performed using the RiboMinus Eukaryote Kit for RNA-Seq (Life Technologies). RNA was quantified with the NanoDrop 2000 spectrophotometer (Thermo Scientific).

5’ RACE and 3’ RACE

For 5’ RACE, RT was performed using a gene-specific reverse primer. The subsequent cDNA was treated with RNase A (Axygen), T1 (ThermoScientific) and H (New England Biolabs), and tailed with dTTP using terminal deoxynucleotidyl transferase (Promega). Nested PCR was performed twice using gene-specific and polyT-specific primers. For 3’RACE, RT was performed using a polyA-specific reverse primer. Nested PCR was performed twice using gene-specific and polyT-specific primers. For both 5’ and 3’ RACE, the cDNA were run on an agarose gel and size selected for fragments between a 100 to 500 base pairs before running the nested

PCR. PCR products were run on an agarose gel, purified and cloned into pGEM-T-Easy vector (Promega) and sequenced.

RT-PCR

For standard RT-PCR, total RNA was reverse transcribed with random hexamers or oligo-dT for 1 hour using AMV-RT (New England Biolabs), M-MLV RT (Promega) or Superscript III (Invitrogen) (Pek, et al., 2012). PCR was carried out using the resulting cDNA. For qPCR, SYBR Fast qPCR kit master mix (2X) universal (Kapa Biosystems, USA) was used with addition of ROX reference dye high and carried out on the Applied Biosystems 7900HT Fast Real-Time PCR system. Oligonucleotides sequences are in Table S1 and reported previously (Pek, et al., 2015).

Statistical analysis

At least 20 germaria from a total of 3 – 5 flies were sampled. Exact number of germaria counted per genotype is indicated in the corresponding figures. Fisher's exact test was performed for all GSC counts. The number of GSCs counted were categorized into two groups, either having >2GSCs or ≤ 2GSCs, or having >3GSCs or ≤ 3GSCs (as indicated by the dotted line in the corresponding figure panels) and subsequently comparing these two groups between the indicated genotypes.

GFP signal quantification

Immunostaining of sample ovaries were carried out in parallel. Images were taken under identical confocal settings and analyzed using ImageJ. Germline cells were identified using Vasa staining. GFP fluorescence intensity was measured at 3 separate areas in the same cell, and an average was taken. This was done for both germline and somatic cells. Upon background subtraction, fluorescence intensities of the germline cells were normalized to somatic cells.

Western blotting

Western blotting was performed as previously described (Wong, et al., 2017; Pek and Kai, 2011). Protein lysates were run on a SDS gel and transferred to a PVDF membrane. Antibodies used were rabbit anti-Mbt (1:500) (Schneeberger and Raabe, 2003), rabbit anti-human FAR1 (1:1000; Sigma-Aldrich, cat. no. HPA017322), and mouse anti-alpha Tubulin (1:10,000; Millipore, Cat. #05-829).

References

Pek, J.W., and Kai, T. (2011). A role for vasa in regulating mitotic chromosome condensation in Drosophila. Curr Biol 21, 39-44.

Pek, J.W., Ng, B.F., and Kai, T. (2012). Polo-mediated phosphorylation of Maelstrom regulates oocyte determination during oogenesis in Drosophila. Development 139, 4505-4513.

Pek, J.W., Osman, I., Tay, M.L., and Zheng, R.T. (2015). Stable intronic sequence RNAs have possible regulatory roles in Drosophila melanogaster. J Cell Biol 211, 243-51.

Schneeberger, D., and Raabe, T. (2003). Mbt, a Drosophila PAK protein, combines with Cdc42 to regulate photoreceptor cell morphogenesis. Development 130, 427-437.

Wong, J.T., Akhbar, F., Ng, A.Y.E., Tay, M.L., Loi, G.J.E., and Pek, J.W. (2017). DIP1 modulates stem cell homeostasis in Drosophila through regulation of sisR-1. Nat Commun 8, 759.